Electronic Supplementary Material (ESI) for CrystEngComm.

Supplementary Information

Surface Oxygen Vacancies of TiO_2 Nanorods by Electron Beam Irradiation for Efficient Photoelectrochemical Water Splitting

Jing Huang[a], Tao Chen[b], Mingyang Zhao[a], Ping Yi[a], Feifan Zhao[a], Bing He[a], Yang Wang[a], Yihuang Chen[c], Xueqin Liu[a], and Zhen Li[a,*]

[a]Engineering Research Center of Nano-Geomaterials of Ministry of Education, Faculty of Materials Science and Chemistry, China University of Geosciences, Wuhan, Hubei, 430074, China

[b]Hubei Key Laboratory of Radiation Chemistry and Functional Materials, Hubei University of Science and Technology, Xianning, Hubei, 437100, China

[c]College of Chemistry and Materials Engineering, Wenzhou University, Wenzhou, Zhejiang 325035, China

*Corresponding authors.

E-mail addresses: zhenli@cug.edu.cn (Z. Li).

Contents

Ⅰ. Calculation

Applied bias photon-to-current efficiency (ABPE)

ABPE were calculated by the equation (1)

$$ABPE = \frac{I(mA \cdot cm^{-2}) \times (1.23 - V_{bias})(V)}{P_{light}(mW \cdot cm^{-2})} \times 100\% \quad (1)$$

where I is the measured photocurrent density at corresponding wavelength, and P_{light} is the measured light power density at that wavelength (100 mW cm^{-2} in this work). V_{bias} is the applied bias between WE and RHE.

Calculation of carrier concentration (*Nd*)

The *Nd* of TiO_2, and EBI-TiO_2 photoanodes through the M-S plots were calculated by the equation (2):

$$Nd = \frac{2}{e\varepsilon\varepsilon_0}\left[\frac{d(1/C^2)}{d\upsilon}\right]^{-1} \quad (2)$$

where ε_0 is the permittivity of free space (8.86×10^{-12} F/m), ε is the dielectric constant of TiO_2, and e is electron charge (1.6×10^{-19} C). and $d(1/C^2)/d\upsilon$ is the slope of the curve shown in M-S plots (**Fig. 6a**).

Charge separation efficiency (η)

The photocurrent (J_{ph}) can be identified as a product of the theoretical photocurrent (J_{abs}) dependent on the light absorption, the charge separation efficiency (η_{sep}), and the interfacial charge transfer efficiency (η_{inj}), which is expressed by the following relation:

$$J_{ph} = J_{abs} \times \eta_{sep} \times \eta_{inj} \quad (3)$$

With the addition of a scavenger (Na_2SO_3), η_{inj} is equal to 1, and thus, η_{sep} can be calculated as the following relationship:

$$\eta_{sep} = \frac{J_{sulfite}}{J_{abs}} \times 100\% \quad (4)$$

$$\eta_{inj} = \frac{J_{ph}}{J_{sulfite}} \times 100\% \quad (5)$$

Ⅱ. Morphology of the photoanodes

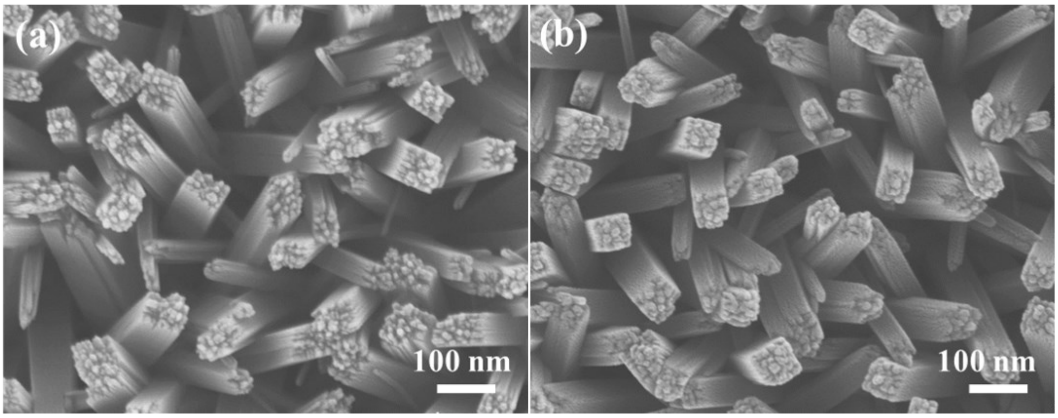

Fig. S1 SEM images of (a) TiO_2 and (b) EBI-TiO_2.

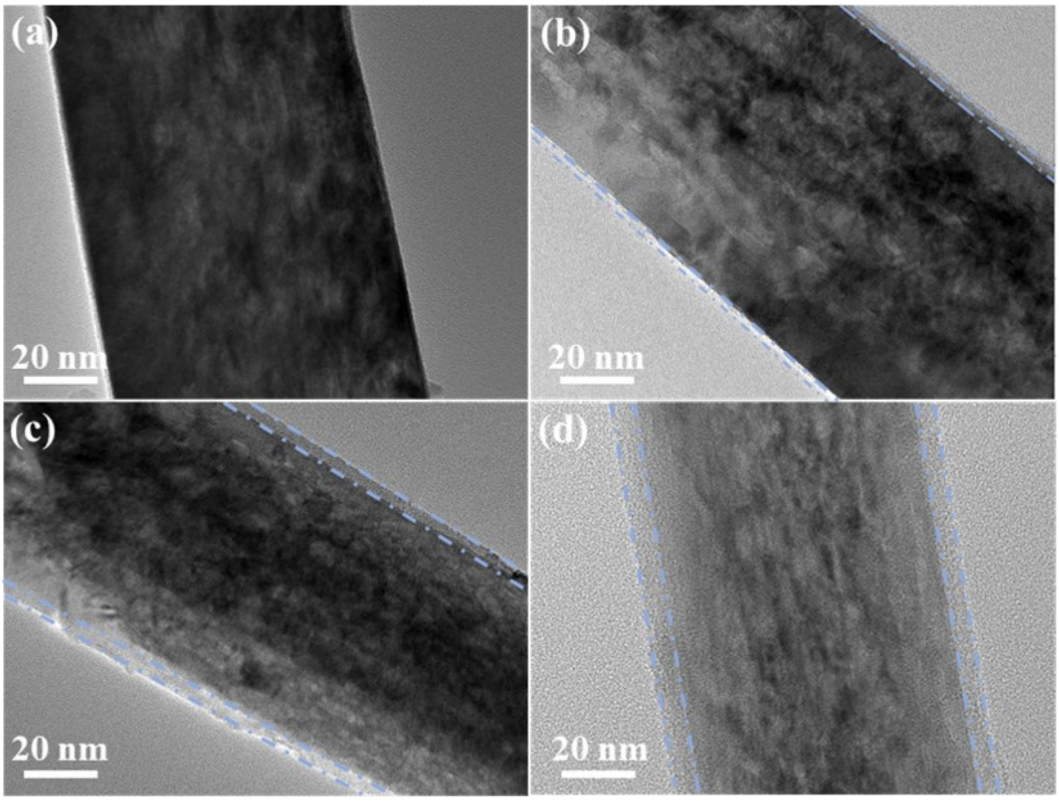

Fig. S2 TEM images of a single nanorod of (a) TiO_2, (b) EBI-TiO_2-15, (c) EBI-TiO_2-30, and (d) EBI-TiO_2-60.

Ⅲ. XPS spectra of the photoanodes

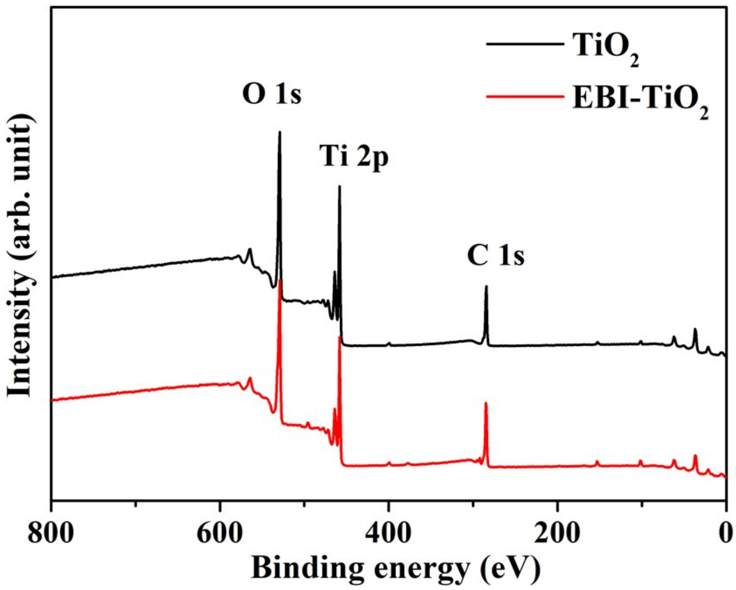

Fig. S3 The survey XPS spectra of TiO_2 and EBI-TiO_2.

Ⅳ. Photoelectrochemical analysis of the photoanodes

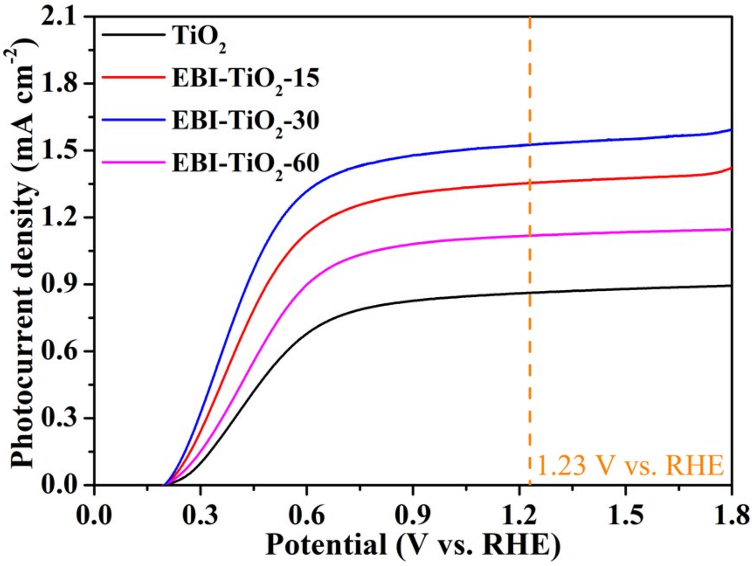

Fig. S4 Photocurrent density-potential (J-V) curves of EBI-TiO_2 with different irradiation dose.

Ⅴ. Light harvesting efficiency and Electron flux of the photoandes

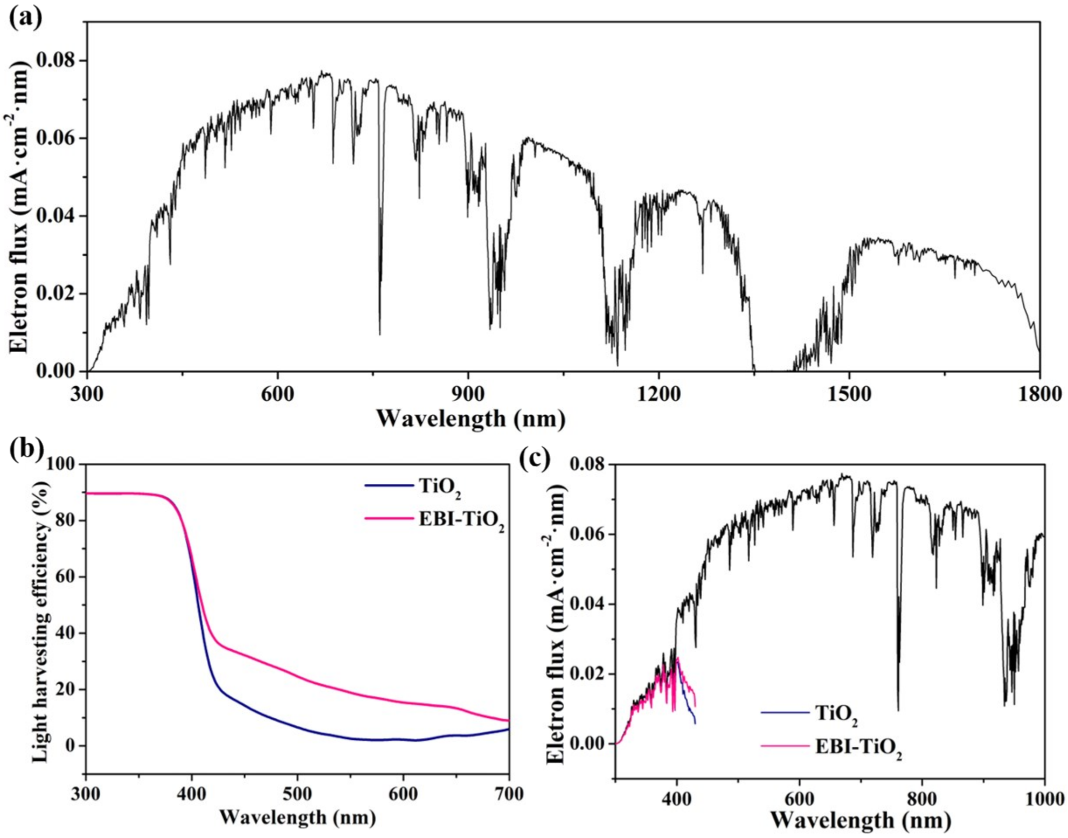

Fig. S5 (a) Electron flux of AM 1.5G solar spectrum. (b) Light harvesting efficiency (η_{LHE}) calculated from the absorption data (η_{ABS}) using the equation η_{LHE} = ($1 - 10^{-\eta_{ABS}}$) × 100%, and (c) Electron flux of TiO_2 and EBI-TiO_2.

Ⅵ. Comparison of J-V curves measured for WO and SO

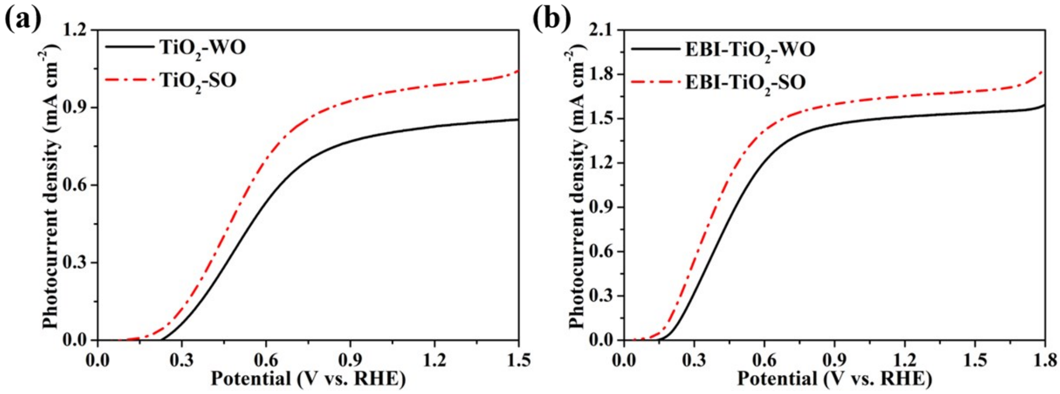

Fig. S6 Comparison of J-V curves measured between (a) TiO_2 and (b) EBI-TiO_2 for water oxidation (WO) in 1 M NaOH solution and sulfite oxidation (SO) measured in 1 M NaOH with 1 M Na_2SO_3 as the hole scavenger under AM 1.5 G illumination. sulfite oxidation.

Ⅶ. Comparison study of PEC performance

Table S1. Comparison of PEC activity of TiO_2-based photoanodes by recently developed V_O generation methods and our EBI approach.

Photoanode material	Methods	Photocurrent density	Test condition	Reference
O&H-Rutile TiO_2/Pd sample	Pd chemical coating, then H_2 reduction	1.5 mA cm^{-2} at 1.23 V_{RHE}	1 M NaOH	[1]
"crystal-deficient" overlayer-TiO_2 NW	solution based lithium reduction	2.0 mA cm^{-2} at 1.23 V_{RHE}	1 M NaOH	[2]
high vacuum annealed TiO_2 NRAs	annealed in high vacuum	2.02 mA cm^{-2} at 0.8 V_{SCE}	0.5 M Na_2SO_4	[3]
TiO_2/STO/r-STO NWs	heated in $NaBH_4$ and Ar flow	0.32 mA cm^{-2} at 1.23 V_{RHE}	1 M KOH	[4]
TiO_2-Ar	annealed in Ar atmosphere	0.98 mA cm^{-2} at 1.23 V_{RHE}	1 M NaOH	[5]
H/TiO_2 nanoarrays	exposed to 10 Torr of H_2 at 400 °C	2.0 mA cm^{-2} at 1.23 V_{RHE}	1 M KOH	[6]
flame-reduced TiO_2 NWs	high temperature (>1000 °C) flame reduction	1.74 mA cm^{-2} at 1.23 V_{RHE}	1 M KOH	[7]
Co-Pi/EBI-TiO_2	electron beam irradiation	1.97 mA cm^{-2} at 1.23 V_{RHE}	1 M NaOH	This work

Ⅷ. Fitting results of Nyquist plots

Table S2. EIS results of the TiO_2 and EBI/Sn:TiO_2 NRs.

Samples	R_s **(Ω)**	R_1 **(Ω)**	***CPE1*** **(μF)**	R_2 **(Ω)**	***CPE2*** **(μF)**
TiO_2	38.59	312.50	0.43	12253.00	32.22
EBI-TiO_2	21.48	68.31	9.32	5691.00	32.32

Ⅸ. References

[1] Y. Xu, C. Zhang, L. Zhang, X. Zhang, H. Yao, J. Shi*, Energy Environ. Sci.*, 2016, **9**, 2410-2417.

[2] *K. Zhang, S. Ravishankar, M. Ma, G. Veerappan, J. Bisquert, F. Fabregat-Santiago, and J. H. Park, Adv. Energy Mater.*, 2017, **7**, 1600923

[3] Yi. Liu, F. Ren , S. She, J. Chen, Y. Fu, G. Cai , X. Wang, Z. Xing, L. Wu, X. Zheng, C Jiang, *Int. J. Hydrogen Energ.*, 2018, **43**, 2057-2063.

[4] Y. He, P. Wang, J. Zhu, Y. Yang, Y. Liu, M. Chen, D. Cao, X. Yan, *ACS Appl. Mater. Interfaces*, 2019, **11**, 37322-37329.

[5] H. Huang, X. Hou, J. Xiao, L. Zhao, Q. Huang, H. Chen, Y. Li, *Catalysis Today*, 2019, **330**, 189-194.

[6] Z. Liang, H. Hou, Z. Fang, F. Gao, L. Wang, D. Chen, W. Yang, *ACS Appl. Mater. Interfaces*, 2019, **11**, 19167-19175.

[7] I. S. Cho, M. Logar, C.H. Lee, L. Cai, F. B. Prinz, X. Zheng, *Nano Lett.*, 2014, **14**, 24-31.